# From Hydrophilic to Superhydrophobic: Fabrication of Micrometer-Sized Nail-Head-Shaped Pillars in Diamond

Mikael Karlsson,* Pontus Forsberg, and Fredrik Nikolajeff

*Department of Engineering Sciences, The Ångström Laboratory, Uppsala University, P.O. Box 534, SE-751 21 Uppsala, Sweden*

The hydrophobicity of microtextured diamond surfaces was investigated. Pillarlike structures were fabricated in both nanocrystalline diamond and microcrystalline diamond. By changing the surface termination of the textured diamond surface, we could switch between superhydrophobic surfaces and hydrophilic surfaces. Examined terminations were hydrogen, fluorine, and oxygen. To evaluate the wetting properties, advancing and receding contact angles were measured. By designing pillars with a wide diamond top on a narrower silicon stem, superhydrophobicity was achieved even when the advancing contact angle on the unstructured diamond surface was below 70°. The possibility to manipulate the hydrophobicity and the Fresnel reflection simultaneously at an infrared wavelength is also demonstrated.

## Introduction

When a liquid comes into contact with a surface that has been micro- or nanostructured, it can either penetrate the structures and wet the whole surface (this is often called the Wenzel state[1]) or it can come to rest on the raised portions of the structure and trap gas in the deeper parts[2−4] (called the Cassie, Cassie−Baxter, or fakir state[5]). In the Wenzel case, the wetting properties are modified by an increase in the wetted surface area, whereas in the Cassie case, the liquid rests on a composite surface composed of solid−liquid and air−liquid interfaces. In both cases, contact line pinning can have a significant effect on the measurable contact angles.[6] To characterize the wetting on such surfaces properly, both advancing and receding contact angles should be measured. High advancing contact angles can be achieved in either state, but low contact angle hysteresis (the difference between the advancing and receding contact angle) is usually seen only in the Cassie state. If the contact angles are high enough and the hysteresis is low, allowing water droplets to roll off easily, the surface is often called superhydrophobic. In nature, such extremely low wettability surfaces can be found, for example, on lotus leaves[7] and the legs of water striders.[8] To achieve the Cassie state, both the geometry and chemistry of the surface must be considered. A high aspect ratio of structures is generally desired.[3] Smaller-structure scales as well as structuring on multiple scales will usually lead to increased stability of the trapped air layer.[9] A very hydrophobic surface chemistry is vital. On a surface of plain pillars, the intrinsic advancing contact angle of the surface material must at the very least be above 90° or capillary forces will suck water into the surface. Even when the contact angle is lower than 90°, for a flat surface, it is in principle possible to design a surface that can support an air film.[10,11] One publication shows that producing such surfaces is possible with nanoscale structures.[12] Superhydrophobic surfaces have gained a lot of interest, both by means of fundamental research and also for industrial applications. Proposed applications include, for instance, self-cleaning surfaces, antifogging surfaces, and low-friction devices in microfluidics. By controlling the wettability, one can change the interaction between a fluid and the surface. For instance, by locally changing the wettability one might be able to block/reduce chemical interaction in the superhydrophobic regions whereas in the hydrophilic region interactions can take place. This could be used on lab-on-a-chip devices (e.g., sensors). For instance, a recent article shows how similar pillar structures, as described in this work, can be very useful for chromatography applications.[13] Surface modification can be of great interest for such devices.

Synthetic diamond exists in several qualities, with a range from nanocrystalline diamond (NCD) and microcrystalline diamond (both are polycrystalline) to the extreme, single-crystalline diamond. During the last few decades, there has been extensive research to increase the quality and growth rate and to lower the deposition temperature. Nowadays fabrication, on a commercial basis and at acceptable growth rates, of high-quality polycrystalline diamond over 6 in. wafers is performed. Even excellent-quality single-crystalline material is now commercially available. This means that diamond has reached a maturity where it starts to reach real applications instead of being just a rare material with a lot of interesting properties but too expensive and exotic to use in industry. Diamond, with its extreme properties such as being the hardest material and having the highest thermal conductivity of all solids and the broadest transmission spectrum, stands out among other materials. It has therefore been suggested that diamond can play the role of a biosensor, mainly because of its chemical inertness but also because one can make it semiconducting

---

*To whom correspondence should be addressed. Phone: +46 18 4717237. Fax: +46 18 4713572. E-mail: mikael.karlsson@angstrom.uu.se.

(1) Wenzel, R. N. *Ind. Eng. Chem.* **1936**, *28*, 988–994.
(2) Bico, J.; Marzolin, C.; Quéré, D. *Europhys. Lett.* **1999**, *47*, 220–226.
(3) Öner, D.; McCarthy, T. J. *Langmuir* **2000**, *16*, 7777–7782.
(4) Yoshimitsu, Z.; Nakajima, A.; Watanabe, T.; Hashimoto, K. *Langmuir* **2002**, *18*, 5818–5822.
(5) Cassie, A. B. D.; Baxter, S. *Trans. Faraday Soc.* **1944**, *40*, 546–551.
(6) Kalinin, Y. V.; Berejnov, V.; Thorne, R. E. *Langmuir* **2009**, *25*, 5391–5397.
(7) Barthlott, W.; Neinhuis, C. *Planta* **1997**, *202*, 1–8.
(8) Gao, X.; Jiang, L. *Nature* **2004**, *432*, 36.
(9) Puukilainen, E.; Rasilainen, T.; Suvanto, M.; Pakkanen, T. A. *Langmuir* **2007**, *23*, 7263–7268.

(10) Lobaton, E. J.; Salamon, T: R. *J. Colloid Interface Sci.* **2007**, *314*, 184–198.
(11) Marmur, A. *Langmuir* **2008**, *24*, 7573–7579.
(12) Lee, S.-M.; Kwon, T. H. *Nanotechnology* **2006**, *17*, 3189–3196.
(13) Eghbali, H.; Verdoold, V.; Vankeerberghen, L.; Gardeniers, H.; Desmet, G. *Anal. Chem.* **2009**, *81*, 705–715.

(electrochemistry, ion-sensitive field effect transistors, etc.)[14,15] and the fact that it is optically transparent (attenuated total reflection elements, etc.).[16] There are also some papers describing how diamond can be used in the human body.[17,18] Recently, a relatively new type of diamond, NCD, has started to find applications for attaching, for instance, DNA and proteins to a surface.[19,20] NCD has turned out to be favorable for functionalization, compared to silicon or gold, mainly because of its stability and good electrochemical properties. There already exist several schemes for making bioactive NCD surfaces for biosensing applications.[21−23]

Superhydrophobic carbon surfaces have been created either by the deposition of amorphous carbon on textured metal[24] or by growing carbon nanotubes[25] (on a flat silicon wafer), followed by the deposition of amorphous carbon nanospheres.[26]

In this article, we show, to the best of our knowledge, for the first time superhydrophobic diamond surfaces. We also show that it is possible to make a surface superhydrophobic by texturing it in the micrometer region, even when the flat surface is hydrophilic. The method is a combination of texturing the diamond surface in a controlled manner on the micrometer level and the chemical termination of the diamond surface. Both NCD and microcrystalline diamond have been used. The evaluated surface terminations are hydrogen, fluorine, and oxygen. The surfaces are evaluated by measuring the advancing and receding contact angles and making X-ray photoelectron spectroscopy (XPS) measurements.

Finally we demonstrate, by using a textured diamond substrate, how it is possible to manipulate the wettability and the surface reflection simultaneously.

### Experimental Methods

**Materials.** Two different types of diamond were used in this study. NCD is a type of diamond with a high content of $sp^3$ bonds and is characterized by having a grain size below 50 nm, regardless of the thickness of the deposited diamond. This means that the surface roughness is generally lower than, for instance, that of microcrystalline diamond. A layer of 1-$\mu$m-thick NCD was deposited on a 4 in. silicon wafer by $\rho$-BeSt coating GmbH (Austria). The NCD layer was characterized with Fourier transform infrared spectroscopy, Raman microspectrometry (NT-MDT NTEGRA Spectra, Russia), and atomic force microscopy (AFM), showing typical parameters for the NCD film with grain sizes between 10 and 15 nm. The spectral profile of the Raman
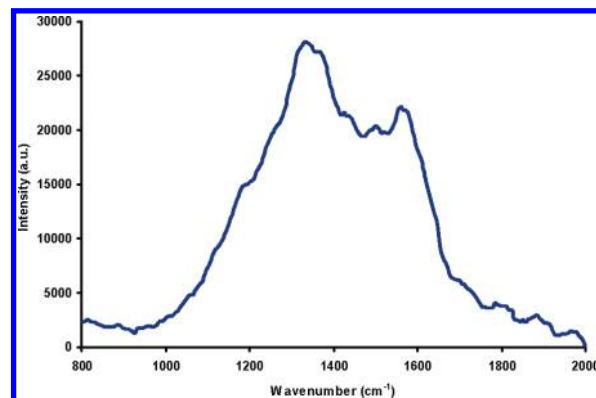
(14) Swain, G. M.; Anderson, A. B.; Angus, J. C. *MRS Bull.* **1998**, *23*, 56–60.

(15) Rezek, B.; Watanabe, H.; Shin, D.; Yamamoto, T.; Nebel, C. E. *Diamond Relat. Mater.* **2006**, *15*, 673–677.

(16) Andersson, P. O.; Lundquist, M.; Tegler, L.; Börjegren, S.; Baltzer, L.; Österlund, L. *ChemPhysChem* **2007**, *8*, 712–722.

(17) Tang, L.; Tsai, C.; Gerberich, W. W.; Kruckeberg, L.; Kandia, D. R. *Biomaterials* **1995**, *16*, 483–488.

(18) Chong, K. F.; Loh, K. P.; Vedula, S. R. K.; Lim, C. T.; Sternschulte, H.; Steinmuller, D.; Sheu, F. S.; Zhong, Y. L. *Langmuir* **2007**, *23*, 5615–5621.

(19) Yang, W.; Auciello, O.; Butler, J. E.; Cai, W.; Carlisle, J. A.; Gerbi, J. E.; Gruen, D. M.; Knickerbocker, T.; Lasseter, T. L.; Russell, J. N.; Smith, L. M.; Hamers, R. J. *Nat. Mater.* **2002**, *1*, 253–257.

(20) Härtl, A.; Schmich, E.; Garrido, J. A.; Hernando, J.; Catharino, S. C. R.; Walter, S.; Feulner, P.; Kromka, A.; Steinmüller, D.; Stutzmann, M. *Nat. Mater.* **2004**, *3*, 736–742.

(21) Nebel, C. E.; Rezek, B.; Shin, D.; Uetsuka, H.; Yang, N. *J. Phys. D: Appl. Phys.* **2007**, *40*, 6443–6466.

(22) Remes, Z.; Choukourov, A.; Stuchlik, J.; Potmesil, J.; Vanecek, M. *Diamond Relat. Mater.* **2006**, *15*, 745–748.

(23) Williams, O. A.; Daenen, M.; D`Haen, J.; Haenen, K.; Maes, J.; Moshchalkov, V. V.; Nesladek, M.; Gruen, D. M. *Diamond Relat. Mater.* **2006**, *15*, 654–658.

(24) Schultz, H.; Leonhardt, M.; Scheibe, H.-J.; Schultrich, B. *Surf. Coat. Technol.* **2005**, *200*, 1123–1126.

(25) Zhang, L.; Resasco, D. E. *Langmuir* **2009**, *25*, 4792–4798.

(26) Shakerzadeh, M.; Teo, H. E.; Tan, C.; Tay, B. K. *Diamond Relat. Mater.* **2009**, *18*, 1235–1238.

(27) Ferrari, A. C.; Robertson, J. *Phys. Rev B* **2001**, *63*, 1–3.

(28) Williams, O. A.; Daenen, M.; D`Haen, J.; Haenen, K.; Maes, J.; Moshchalkov, V. V.; Nesladek, M.; Gruen, D. M. *Diamond Relat. Mater.* **2006**, *15*, 654–658.



**Figure 1.** Raman spectrum of an NCD film.

spectrum viewed in Figure 1 agrees well with literature data on nanocrystalline diamond.[27,28] The shoulder at 1180 cm$^{-1}$ is attributed to $sp^2$-bonded carbon atoms, the peak at 1332 cm$^{-1}$ is attributed to diamond (tetrahedral coordinated carbon), and the peak at 1560 cm$^{-1}$ is attributed to the well-known G band in disordered carbon. Typical surface roughness values were 7−10 nm rms. The NCD film was deposited with hot filament methods. The other type of diamond used was microcrystalline diamond of optical quality. We used free-standing diamond substrate, 10 mm in diameter and 300 $\mu$m in thickness, from Element Six Ltd. (U.K.). The surface is polished to a surface roughness of 10−15 nm rms, and typical grain sizes are between 30 and 70 $\mu$m. This type of diamond is grown by microwave-assisted chemical vapor deposition. Though the NCD has a lower rms-roughness, the high frequency means that it is still the rougher of the two for wetting properties.

**Textured NCD Surface.** The NCD wafer was first cleaned for 10 min in hot $H_2SO_4/H_2O_2$ (piranha). The wafer was subsequently coated with a 1-$\mu$m-thick aluminum (Al) layer by sputtering (Von Ardenne CS 730S). By using standard photolithography (Karl Süss mask aligner), a resist pattern was fabricated on top of the Al-coated wafer. The pattern was then etched into the Al layer by inductively coupled plasma (ICP) etching using $Cl_2/BCl_3/Ar$ chemistry (Plasmatherm SLR). The Al layer could then be used as a mask for NCD etching. The same ICP system was employed for this etching using $O_2/Ar$ chemistry. For a more detailed description of the process used, see ref 29. By changing the plasma process to the so-called Bosch process,[30] pillars consisting of silicon with NCD/Al on top were fabricated. The process is performed in three steps that are repeated several times, depending on how deep one wants to etch. The first step is a polymer deposition process, and the second step is a polymer etch step where all of the deposited polymer is etched away except on the sidewalls. In the third step, the silicon etching step, silicon is etched but not the polymer. This means that high aspect ratio structures can be etched using the Bosch process. The chemistry is a combination of $C_4F_8/SF_6/Ar$. As a final etching step, an isotropic silicon etch was used (i.e., using the third step in the Bosch process). In this way, an undercut of the NCD squares can be fabricated. Finally, Al was etched away in an aluminum wet etch (phosphoric acid, water, and nitric acid).

**Textured Microcrystalline Diamond.** The CVD diamond substrate was cleaned, Al coated, and lithographically patterned in the same way as described for the NCD wafer. The only difference is that we use a 2-$\mu$m-thick Al layer because the etching process for diamond is much more aggressive than that for silicon. (The diamond etching process also attacks Al at a slow rate.) The square pattern was etched into the diamond by the same methods as for the NCD etching, with the difference that here we etched to the desired depth in the diamond (pure diamond substrate).

(29) Karlsson, M.; Nikolajeff, F. *Opt. Express* **2003**, *11*, 502–507.

(30) Laermer, F.; Urban, A. *Microelectron. Eng.* **2003**, *67−68*, 349–355.

Finally, we stripped the Al layer using the same acid mixture as above. For the microcrystalline substrate, we have a textured surface in pure diamond, whereas the NCD structures are a hybrid of NCD and silicon.

This type of pillar structure (2D grating) can also be used as a so-called antireflection (AR) structure. When a grating period becomes substantially smaller than the illuminating wavelength, all of the light will be transmitted into the zeroth transmission order (i.e., no deviation of the light). Depending on the grating's depth and geometry, one can synthesize an appropriate refractive index distribution so that the surface (Fresnel) reflection is reduced. See ref 29 for a general discussion of subwavelength gratings in diamond. The subwavelength grating was designed to reduce surface reflections using a commercial optics computer program (GSOLVER, Grating Solver Development Company). This program uses algorithms that solve the vector Maxwell equations in the grating region. With a fill factor of 0.25 (duty cycle 0.5) and a grating depth of 9 $\mu$m, the calculated Fresnel reflection from one diamond surface was reduced from 17 to 4% at a wavelength of 45 $\mu$m.

**Surface Termination.** The normal state (i.e., as grown) for diamond is when the carbon atoms at the surface bond to a hydrogen atom. However, using our methods for texturing the diamond, the termination has to be considered unknown, most probably a combination of hydrogen (C−H) and oxygen termination (C−O or C−OH). For the structured NCD surface, there might also be some residues of fluorocarbons on the side walls of the pillars originating from the Bosch process. However, most of these residues are probably removed when the Al layer is stripped. Before the surface treatments, all samples (flat and textured) were cleaned in hot piranha for 10 min. All samples were then oxygen terminated both to clean them and to give a consistent, highly hydrophilic starting point for all samples.

Oxygen termination was accomplished by using oxygen plasma[31,32] (Tepla 300). The parameters used were as follows: pressure, 100 mTorr; oxygen flow, 100 sccm; microwave power, 1000 W; processing time, 10 min.

Hydrogen termination was accomplished by using a hot filament chemical vapor deposition (CVD) system (Nova Diamant, Sweden) designed for the fabrication of polycrystalline diamond. The diamond substrates were placed in the CVD chamber with a hot filament temperature of 2000 °C, a substrate temperature of 800 °C, and a pressure of 35 mbar for 20 min in a pure hydrogen atmosphere.[20] The system was then cooled for 30 min under constant hydrogen flow.

The success of the oxygen and hydrogen surface terminations was validated with contact angle measurements.

Fluorine termination was achieved using $C_4F_8/SF_6/Ar$ plasma. The diamond substrate was placed in the ICP system using the following process parameters: ICP power, 825 W; bias, −90 V; $C_4F_8$ flow, 2 sccm; $SF_6$ flow, 100 sccm; Ar flow, 30 sccm; pressure, 23 mTorr; processing time, 30 s. In the literature, there are reports of the fluorine termination of diamond by plasma treatment in fluorine-containing gases.[31,32] However, one group reports that similar plasma treatment yields the formation of a very thin fluorocarbon layer (< 1 nm) on carbon-containing surfaces.[33,34] To investigate whether the fluorine treatment yields the deposition of an unwanted fluoropolymer, a silicon and a silicon oxide substrate were placed together with the diamond substrates during the fluorination experiment.

The long-term stability of hydrogen- and fluorine-terminated diamond surfaces is good. For instance, one group shows that the contact angles are stable (decrease of 2 to 5°) over 1 year.[32]

However, the oxygen-terminated surface is considered not to be as stable over time. Normally, one can see an increase in the contact angle of about 20−30° after some months. After that, the contact angle seems to stabilize.[32]

The obtained surface chemistry for the fluorine termination was investigated by XPS using a PHI Quantum 2000 instrument with monochromatized Al K$\alpha$ radiation.

**Contact Angle Measurements.** Contact angles were measured by the sessile drop technique using distilled water. A small droplet (2−4 $\mu$L) attached to the end of a syringe needle was placed on the surface. To measure the advancing and receding angles, water was added to or withdrawn from the droplet until the wetting line was seen to move. Pictures were taken of the (backlit) droplets by a horizontal microscope with an attached video camera. Contact angles were then extracted from the pictures using the DropSnake plug-in[35] for ImageJ. On surfaces with very high contact angles, the method of expanding and contracting droplets can be impractical because of the rather large volume increases required to observe the clear movement of the contact line. Instead, the droplet was slowly dragged across these surfaces by moving the surface horizontally, perpendicular to the camera direction while the droplet stayed attached to the syringe needle. Advancing and receding angles were then recorded from the same picture. For each surface, contact angles were averaged over at least 10 measurements.

## Results and Discussion

**NCD Surface.** Silicon pillars, with 1-$\mu$m-thick NCD on top of the pillar, were fabricated using ICP etching in oxygen and argon chemistry, followed by fluorine ICP etching. The pillars were set in a 2D square array of $5 \times 5 \ \mu m^2$ pillars with periods of 9, 10, 14, and 19 $\mu$m; this means that we have fill factors of 0.31, 0.25, 0.13, and 0.07. Each pattern covers an area of 1 cm$^2$. The etched depth was 11−15 $\mu$m with the lower value associated with the denser patterns as a result of a somewhat lower etch rate. An undercut of the NCD layer was created by tuning the fluorine etching process to a more isotropic etch. The isotropic silicon etch was used either at the beginning or at the end of the silicon etching. This isotropic etch was used to etch about 1 to 2 $\mu$m of silicon. Figure 2 shows scanning electron microscope (SEM) pictures of fabricated NCD/silicon pillars.

The process generates fairly well defined pillars, and the ripple on the sidewalls originates from the anisotropic Bosch process. This ripple decreases or almost disappears when the isotropic process is used afterwards. The main reason for the rounded squares is that we have quite a rough NCD material, which makes the photolithography somewhat difficult, especially when working with small feature sizes.

**Optical Diamond.** The diamond pillars were etched to a height of about 9 $\mu$m. The same chromium photomask was used in the photolithography as for the NCD pillars with a 10 $\mu$m period. Because the crystallite size in the diamond sample is an order of magnitude larger than the pillars, the pillars can be considered to be effectively single-crystalline, with at most one grain boundary. In Figure 3, one can see the fabricated diamond pillars.

Figure 3 shows that the dimensions of the squares have decreased from $5 \times 5 \ \mu m^2$ to approximately $4 \times 4 \ \mu m^2$. The main reason for this decrease in square size and also the rather nonsharp structures is that we used standard contact photolithography on a small substrate. The edge bead gives rise to a gap between the chromium photomask and the substrate during exposure, and because of the diffraction of light, the above-mentioned problem occurs. One can overcome this problem by using e-beam lithography[26] or larger substrates. However, it is reasonable to believe

(31) Popov, C.; Kulisch, W.; Bliznakov, S.; Ceccone, G.; Gilliland, D.; Sirghi, L.; Rossi, F. *Diamond Relat. Mater.* **2008**, *17*, 1229–1234.

(32) Kulisch, W.; Popov, C.; Gilliland, D.; Ceccone, G.; Sirghi, L.; Ruiz, A.; Rossi, F. *Diamond Relat. Mater.* **2009**, *18*, 745–749.

(33) Schvartzman, M.; Wind, S. J. *Nanotechnology* **2009**, *20*, 1–7.

(34) Schvartzman, M.; Mathur, A.; Hone, J.; Jahnes, C.; Wind, S. J. *Appl. Phys. Lett.* **2008**, *93*, 1–3.

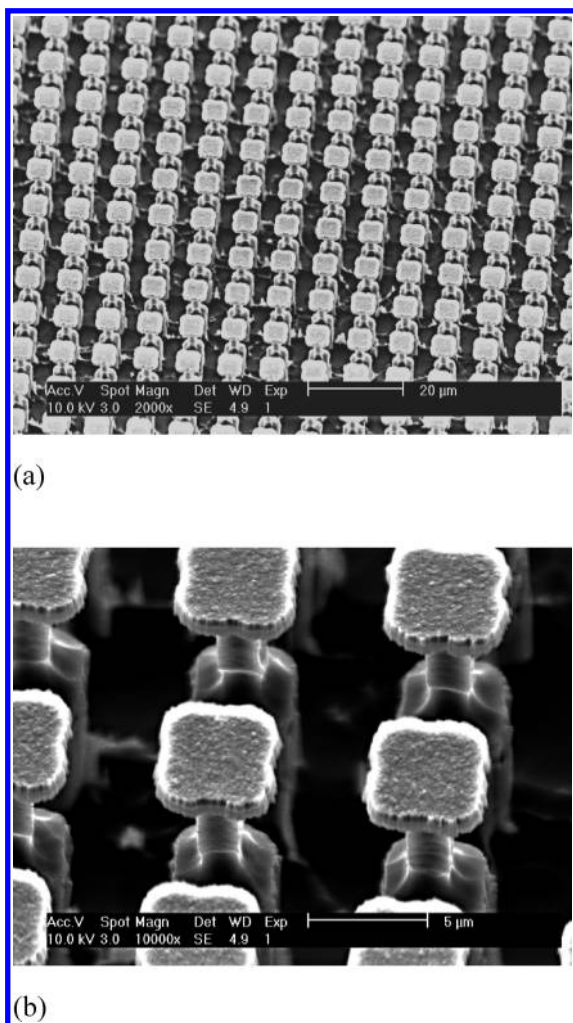(35) Stalder, A. F.; Kulik, G.; Sage, D.; Barbieri, L.; Hoffman, P. *Colloid Surf., A* **2006**, *286*, 92–103.

**Figure 2.** (a) SEM picture of NCD/silicon pillars fabricated by isotropic etching followed by anisotropic etching. (b) Close-up picture of the pillars.
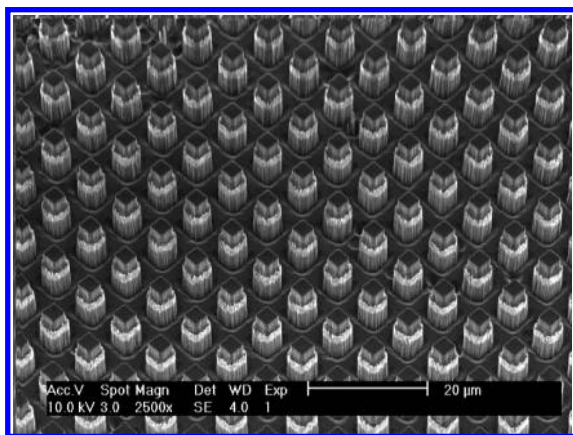


**Figure 3.** SEM picture of diamond pillars in a CVD diamond of optical quality.

that these types of structures give in principle, with respect to wettability, the same result.

These diamond pillars were also designed to reduce surface reflections.

**XPS Measurements.** Figure 4 shows the XPS spectrum of the fluorine-terminated diamond surface. Sputtering was not used prior to the measurement. The observed peaks are from carbon
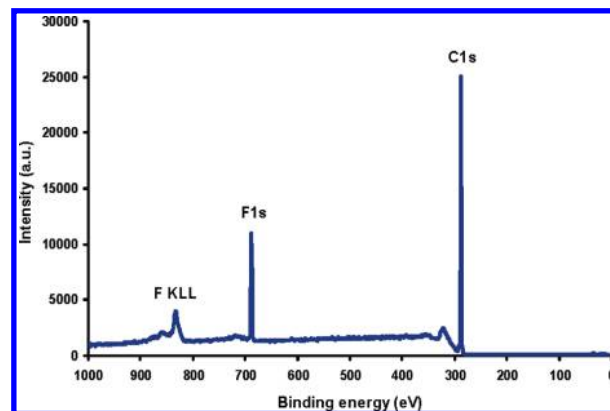


**Figure 4.** XPS spectrum of the fluorine-terminated diamond surface.

(C 1s) and fluorine (F 1s), and by using the peak areas together with the bulk sensitive factors the compositions of fluorine and carbon were calculated to be 16 and 84%, respectively. The fluorine KLL Auger peak is also viewed in the XPS spectrum. This clearly indicates that the fluorination of the diamond surface has been successful.

Hydrogen is not detectable with XPS, and hydrogen termination was confirmed by the high contact angles of the treated surface (close to 70°). In the same way, the success of the oxygen termination was shown by the high wettability of the terminated surface (contact angle close to zero).

**Contact Angle Measurements.** To characterize the wetting properties, advancing and receding contact angles were measured in this study. Both structured and unstructured samples were terminated with hydrogen, fluorine, and oxygen. Pieces of flat silicon and, in the case of fluorine treatment, also a silicon oxide surface were treated at the same time as the diamond samples. After surface modification, the contact angles were measured within 8 h. Results of the measurements on the diamond samples are presented in Figures 5 and 6. On the flat surfaces, we see that on both the nanocrystalline and microcrystalline diamonds the fluorine termination gave the most hydrophobic surface with advancing contact angles well above 100°. On the hydrogen-terminated surfaces, the measured contact angles were consistently below 90°. With both terminations, large contact angle hysteresis was observed on the nanocrystalline samples. This is most likely due to the roughness of the nanocrystalline surface giving rise to the pinning commonly seen in Wenzel wetting. The chemical heterogeneity introduced by the grain boundaries could also play a role in increasing hysteresis.[36] On the microcrystalline samples with a lower roughness and fewer grain boundaries, much lower contact angle hysteresis was observed. On the smooth silicon surfaces, the hydrogen treatment gave rise to a 60° advancing contact angle and a 26° receding contact angle.

Fluorine treatment gave a 67° advancing angle on silicon and a 43° advancing angle on silicon oxide; the receding angle was below 10° for both. These angles are not much different from those measured before the treatment, showing that on these surfaces no film is deposited. This hints that the diamond surface is terminated with fluorine rather than being coated with a fluoropolymer film.

On the textured surfaces, we saw typical Cassie behavior on the fluorine-terminated surfaces of both the nanocrystalline and microcrystalline samples with advancing contact angles of around 160°. This is not surprising considering the high contact angles on the flat samples. In the case of hydrogen termination, however,

(36) Priest, C.; Rossen, R.; Ralston, J. *Phys. Rev. Lett.* **2007**, *99*, 1–4.
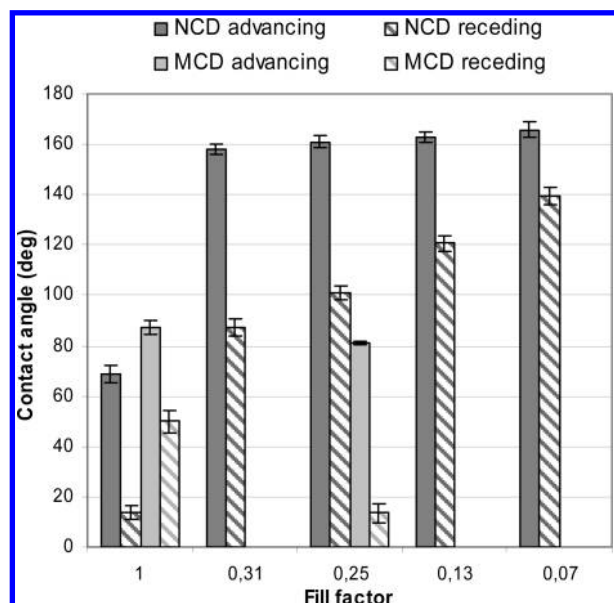
**Figure 5.** Advancing and receding contact angles for hydrogen-terminated micro- and nanocrystalline diamond surfaces. Values are presented for flat and textured surfaces with different fill factors.

the microcrystalline diamond pillars were not hydrophobic enough to support a droplet in the Cassie state. Instead, water was pulled down into the structure, and the lower contact angles and large hysteresis expected of the Wenzel state were observed. On the nanocrystalline diamond, however, the nail-head-shaped tops of the pillars now come into play and hold the droplet up despite the hydrophilic nature of the diamond. The reason for this is that the water needs to wet the underside of the head before penetrating down along the pillars, raising the effective contact angle by 90° as described by Lobaton and Salamon.[10] The disadvantage of this design is that the Cassie state becomes very sensitive to imperfections in the pattern. If water can penetrate into the underlying silicon structure at even a single point, for example, because of a broken pillar top, then it is enough to pull the whole droplet down to stick in the Wenzel state. This was sometimes seen during the measurements as the droplet was dragged onto a damaged part of the pattern. The receding angles on both the fluorine- and hydrogen-terminated nanocrystalline samples decreased with pillar density, as expected when the contact line has a longer fraction in contact with the solid surface on which to pin. The highest receding contact angles (and the lowest hysteresis) in this study were measured on the fluorine-terminated microcrystalline sample. Although the pillar density on this sample was relatively large (with an approximately 25% fill factor), the smoothness of the surface allowed the contact line to de-pin easily from the pillars.

For the oxygen-terminated diamond surfaces, both flat and textured, the contact angles were zero or so close to zero that an accurate value could not be measured using the sessile drop technique. The oxygen-treated silicon surface was also completely wetted.

The structured microcrystalline diamond substrate was evaluated in the IR region with a spectrophotometer (Perkin-Elmer). For the transmission measurements, we used a pinhole with a diameter of 6 mm to reduce the beam width because the size of the AR-structured area is 8 mm in diameter. The surface reflection is reduced from 17% for the blank diamond to 5% for the structured diamond (the calculated value from GSOLVER is
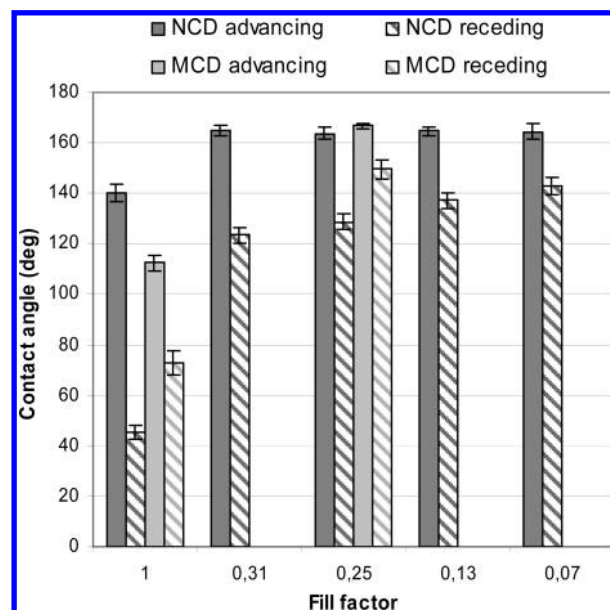


**Figure 6.** Contact angles for fluorine-terminated micro- and nanocrystalline diamond surfaces.

4%) at a design wavelength of 45 $\mu$m. It is noticeable that the surface reflection is significantly reduced from the wavelength of 25 $\mu$m up to 50 $\mu$m.

## Conclusions and Future Work

Microtextured diamond surfaces were fabricated with the aim of reaching the superhydrophobic state. Both NCD and microcrystalline diamond were used. The diamond surfaces were terminated with oxygen, hydrogen, and fluorine to enhance the wetting properties. By using fluorine termination, both textured NCD and textured microcrystalline diamond were made superhydrophobic. For NCD and microcrystalline diamond, advancing contact angles of 160 and 165° and hysteresis values of 17 and 15°, respectively, were measured. To produce a superhydrophobic surface using hydrogen-terminated diamond, a nail-head-shaped pillar design was needed. When the diamond surfaces were oxygen terminated, the surface was completely wetted (i.e., superhydrophilic). We conclude that diamond can be made superhydrophobic without adding a film or other material to the surface.

Clearly, we have been able to drastically increase the optical transmission in the IR regime and the hydrophobicity of diamond simultaneously. Future studies will include AR treatment in the visible/near-IR region combined with superhydrophobic surfaces.

**Note Added after ASAP Publication.** This article was released ASAP on September 23, 2009. Text was added to the fifth paragraph of the Surface Termination section, and the correct version was posted on October 7, 2009.